Advances in Water Resources 115 (2018) 88–94

Contents lists available at ScienceDirect

Advances in Water Resources

journal homepage: www.elsevier.com/locate/advwatres

Estimation of relative permeability and capillary pressure from mass imbibition experiments

Nayef Alyafei[a,*], Martin J. Blunt[b]

[a] Department of Petroleum Engineering, Texas A&M University at Qatar, Qatar
[b] Department of Earth Science and Engineering, Imperial College London, Qatar Carbonates and Carbon Storage Research Centre, SW7 2AZ, United Kingdom

ARTICLE INFO

Article history:
Received 12 October 2017
Revised 23 February 2018
Accepted 2 March 2018
Available online 6 March 2018

Keywords:
Spontaneous imbibition
Capillary dominated flow
Relative permeability
Capillary pressure
Semi-Analytical solution

ABSTRACT

We perform spontaneous imbibition experiments on three carbonates - Estaillades, Ketton, and Portland - which are three quarry limestones that have very different pore structures and span wide range of permeability. We measure the mass of water imbibed in air saturated cores as a function of time under strongly water-wet conditions. Specifically, we perform co-current spontaneous experiments using a highly sensitive balance to measure the mass imbibed as a function of time for the three rocks. We use cores measuring 37 mm in diameter and three lengths of approximately 76 mm, 204 mm, and 290 mm. We show that the amount imbibed scales as the square root of time and find the parameter C, where the volume imbibed per unit cross-sectional area at time t is $Ct^{1/2}$. We find higher C values for higher permeability rocks. Employing semi-analytical solutions for one-dimensional flow and using reasonable estimates of relative permeability and capillary pressure, we can match the experimental data. We finally discuss how, in combination with conventional measurements, we can use theoretical solutions and imbibition measurements to find or constrain relative permeability and capillary pressure.

1. Introduction

Spontaneous water imbibition is the invasion of the water into a porous medium due to capillary forces and can only occur in water-wet and mixed-wet systems (Morrow and Mason, 2001). Spontaneous imbibition, SI, has two modes: co-current and counter-current, see Fig. 1. Counter-current imbibition occurs when the oil and brine flow in opposite directions from the same inlet, whereas co-current is when the brine and oil flow in the same direction. The rate of water imbibition into the porous medium is a function of permeability, relative permeability, capillary pressure, initial water saturation, boundary conditions, viscosity, interfacial tension, and wettability (Graue and Fernø, 2011; Mason and Morrow, 2013; Zhang et al., 1996). Spontaneous imbibition is an important recovery mechanism in naturally and artificially induced fractured reservoirs (Morrow and Mason, 2001). In addition, imbibition is the process rendering carbon dioxide immobile in the process of carbon capture and storage (CCS) (Alyafei and Blunt, 2016). Recently, the use of imbibition experiments to estimate multi-phase flow parameters such as relative permeability and capillary pressure has been proposed (Alyafei et al., 2016; Haugen et al., 2014; Li and Horne, 2005).

Several studies proposed analytical solutions for spontaneous imbibition (Cil, 1996; Kashchiev and Firoozabadi, 2003). However, these solutions made additional assumptions that were not physically valid. In contrast, the solution derived by Schmid et al. (2016, 2011) based on the work of McWhorter and Sunada (1990, 1992) is a general solution applicable for any combination of relative permeability and capillary pressure. A detailed mathematical description of this solution is provided elsewhere (Alyafei et al., 2016; Schmid et al., 2016). For co-current flow, the conservation equations can be expressed as:

$$(F - f)F'' = -\frac{\phi}{2C^2}D \tag{1}$$

and for counter-current flow:

$$FF'' = -\frac{\phi}{2C^2}D \tag{2}$$

where

$$D(S_w) = -\frac{k\lambda_w\lambda_{nw}}{\lambda_t}\frac{\partial P_c}{\partial S_w} \tag{3}$$

is the non-linear dispersion coefficient [m^2/s], F is the capillary dominated fractional flow, F'' is the second derivative of the capil-

* Corresponding author.
E-mail address: nayef.alyafei@qatar.tamu.edu (N. Alyafei).

https://doi.org/10.1016/j.advwatres.2018.03.003

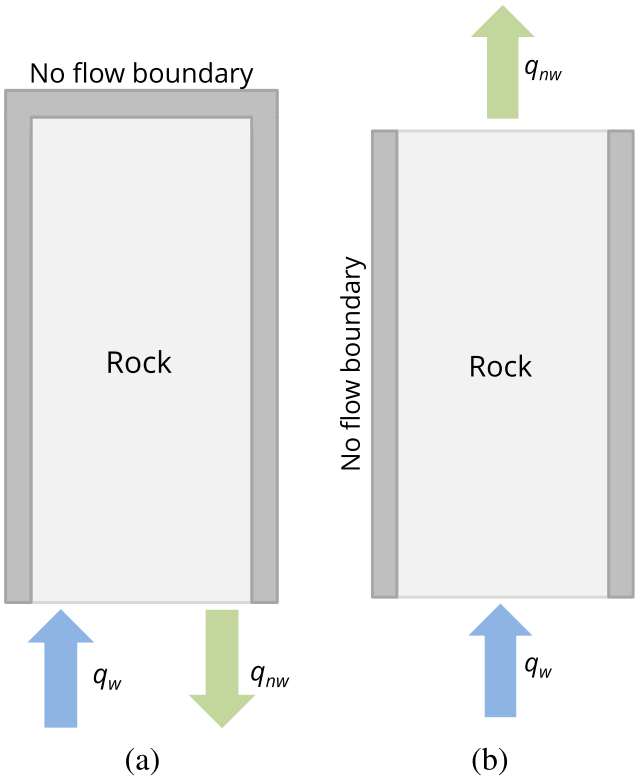

Fig. 1. Schematic representing spontaneous imbibition under (a) counter-current and (b) co-current conditions. The subscripts *w* and *nw* indicate wetting and non-wetting phase respectively.

lary dominated fractional flow, ϕ is porosity, C is a constant that quantifies the rock's ability to imbibe [m/$\sqrt{s}$], f is the Buckley–Leverett fractional flow, λ_w is the wetting phase mobility [1/Pa.s], λ_{nw} is the non-wetting phase mobility [1/Pa.s], λ_t is the total mobility [1/Pa.s], and $\partial P_c/\partial S_w$ is the derivative of the capillary pressure with respect to saturation [Pa].

The volume of water imbibed per unit area per unit time, $q_w(t)$, is defined as:

$$q_w(t) = 2C\sqrt{t} \tag{4}$$

where C is the imbibition constant [m/$\sqrt{s}$], and t is time [s].

Schmid et al. (2016, 2011) presented the formal solution to the co-current flow as:

$$F = \iint \frac{-\phi}{2C^2}\frac{D}{(F-f)}d^2S_w \tag{5}$$

and similarly with f=0 for counter-current flow. This equation is implicit in F and so can only be solved iteratively. Open source spreadsheets have been provided to analyze the semi-analytical solution for co-and counter-current spontaneous imbibition and can be found here (Alyafei et al., 2016; Schmid et al., 2016). The resultant solution is a function of both imbibition relative permeability and capillary pressure which is different than the Buckley–Leverett solution for flow with an imposed pressure difference which is a function of relative permeability only.

Note the solution assumes that the amount imbibed scales as the square root of time. In addition, it is only valid at early time where the flow is entirely governed by capillary forces in the absence of constraining boundaries (Li and Horne, 2001; Olafuyi et al., 2007; Suzanne et al., 2003). The late time is governed by boundary/diffusion where the water front reaches the boundary and the recovery rate decays exponentially.

In this paper, we will address the following:

- Examine the validity of using $\sqrt{t}$ as a scaling parameter and observe the imbibition behavior on different rocks with varying lengths.
- Provide a procedure to obtain the C constant from mass imbibition data and discuss its application.
- Develop an understanding of spontaneous imbibition of uniformly water-wet media experimentally and compare it with the semi-analytical solution.
- Discuss how to use spontaneous imbibition experiments, in combination with other, more traditional measurements, to determine imbibition capillary pressure and relative permeability.

In addition, this paper gives a systematic procedure to extract imbibition relative permeability and capillary pressure from simple mass imbibition experiments.

2. Experimental procedure

2.1. Rocks

We use three carbonate rocks in our study. Estaillades is a bioclastic limestone, which contains 99% calcite ($CaCO_3$) and traces of dolomite and silica and comes from France (Wright et al., 1995). The measured porosity of Estaillades ranges from 27.5–28.2% with permeability 1.19–3.94 $\times$ 10^{-13} m^2. Ketton is an oolitic limestone of 99.1% calcite and 0.9% quartz and comes from the UK Ashton (1980). The porosity ranges from 20.5–23.4% and the permeability from 1.37–2.54 $\times$ 10^{-12} m^2. Portland is a skeletal-peloidal limestone of 96.6% calcite and 3.4% quartz and comes from the UK (Brenchley and Rawson, 2006). The porosity ranges from 16.1–20.0% and the permeability from 0.65–3.5 $\times$ 10^{-14} m^2. In our study, we use cores measuring 37 mm in diameter and three lengths of approximately 76 mm, 204 mm, and 290 mm, two samples of each length were studied to assess experimental reproducibility. Table 1 shows further geological information about the rocks used. Fig. 2 shows the measured mercury injection capillary pressure (MICP) of samples of the three rocks using an Autopore IV 9520 measured at Weatherford Laboratories in East Grinstead, UK. We can see that Portland has the highest capillary entry pressure (minimum value of $P/2\sigma\cos\theta$) of approximately 0.18 μm^{-1}, while Estaillades has a lower capillary entry pressure of approximately 0.029 μm^{-1}. Ketton has the lowest capillary entry pressure of approximately 0.017 μm^{-1}.

Table 1
Geological information about the rocks used in this study.

Rock	Geological group	Geological age	Age [million years]	Locality
Estaillades.	Estaillade Formation	Upper Cretaceous	72-100	Oppede, France
Ketton	Lincolnshire Formation	Middle Jurassic	169–176	Rutland, UK
Portland	Portland Formation	Upper Jurassic	145-152	Portland, UK

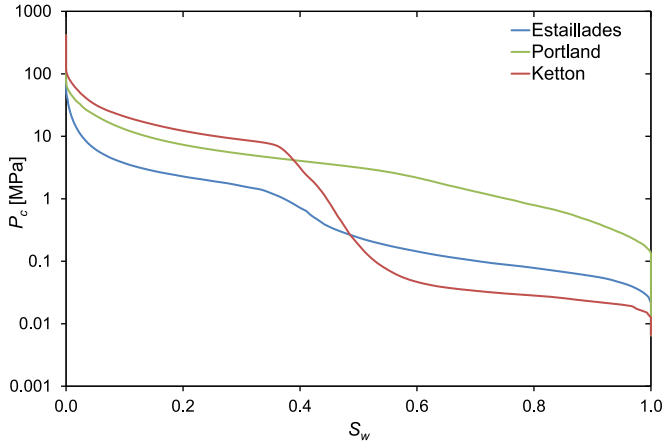

Fig. 2. Measured capillary pressure (mercury/air) as a function of equivalent water saturation.

2.2. Fluids and conditions

We conduct our experiments at ambient conditions of atmospheric pressure and room temperature of 20 ± 1 °C. We use air as the non-wetting phase and brine, with 5 wt. % sodium chloride (NaCl) and 1 wt. % potassium chloride (KCl) mixed with deionised water, as the wetting liquid phase. In addition, we equilibrate the brine with the carbonate samples for 48 h by mixing them using magnetic stirrer to eliminate any reaction between the brine and the rock surface which might alter the rock morphology. Then, we leave the brine for additional 48 hours to settle and finally we filter it, using a fine filter paper, to remove the particles that might block the flow pathways of the rocks.

The density of brine is 1,040.8 kg/m^3 measured using Anton Paar DMA 5000 M and the viscosity is reported as 1.0085 mPa s (Lide, 2004). The air/brine interfacial tension is 0.073 N/m measured using Ramé-Hart model 590 device and the air viscosity is reported as 0.0018 mPa s (Tavassoli et al., 2005).

2.3. Mass imbibition

Before we start the SI experiment, we perform our routine analysis by taking the dimensions of the core, measuring the dry weight of the core, and measuring the helium porosity. However, we use the mass balance technique to measure the porosity for the 204 mm and 209 mm length cores, where we take the dry weight and compare it to the fully saturated core with degassed brine after the experiments, since the helium porosimeter cell is too small to fit them.

We measure the permeability of the core using either gas before starting the spontaneous imbibition experiment, or brine after finishing the spontaneous imbibition experiment and measuring the fluid saturation, where we use a Hassler type cell with a cylindrical confining fluid. We use three cell lengths to fit our different core lengths.

To start our SI experiment, we apply heat shrink wrapping to confine the outer boundaries of the core and make sure that only co-current imbibition is applied. Then, we weigh the core again with the heat shrink and after that we attach the core to a Mettler Toledo XP5003S balance with 0.001 g accuracy and we lift the brine reservoir at the bottom of the core surface to be in contact with the core, Fig. 3. Before that moment, we start recording the weight changes over time as the balance is connected to the computer. We have three recording settings; we record 10 points per second, 5 points per second, and 2 points per second. We use the 10 points per second for Ketton, as it has the highest permeability

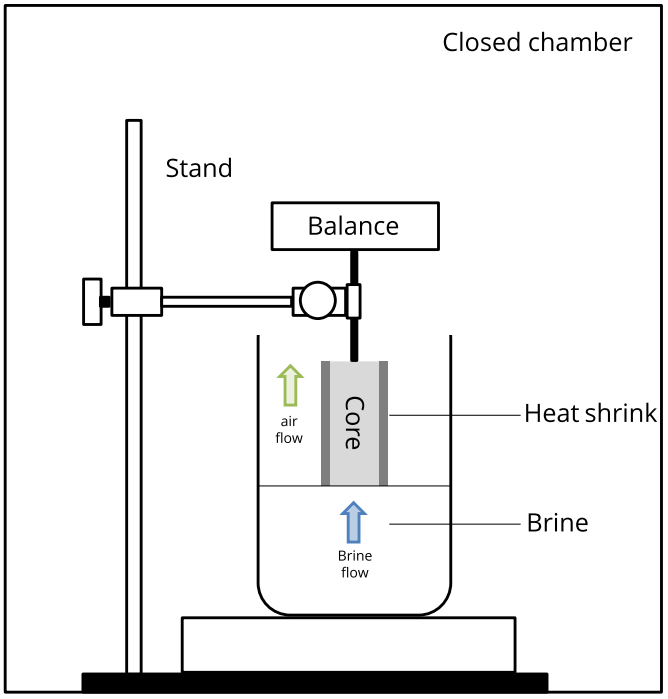

Fig. 3. Schematic of the experimental apparatus for ambient condition co-current spontaneous imbibition, where the mass of brine imbibed into a rock fully saturated with air is measured as a function of time.

Table 2
Summary of the petrophysical properties measured for the rocks used in mass imbibition experiments. E, K, and P denote Estaillades, Ketton, and Portland respectively.

Core Label	D [mm]	L [mm]	ϕ [%]	k [m^2]	S_{gr}
E1	37.8	76.3	28.0	1.34×10^{-13}	0.29
E2	37.8	76.3	27.8	3.53×10^{-13}	0.28
E3	37.9	204.0	27.5	1.19×10^{-13}	0.25
E4	37.9	204.0	27.5	1.55×10^{-13}	0.25
E5	37.9	292.0	28.2	3.94×10^{-13}	0.23
E6	37.9	293.0	28.0	3.28×10^{-13}	0.23
K1	37.8	76.0	23.4	1.62×10^{-12}	0.35
K2	37.8	76.3	20.5	1.37×10^{-12}	0.27
K3	38.1	205.0	23.2	1.88×10^{-12}	0.34
K4	38.0	205.0	21.7	1.99×10^{-12}	0.28
K5	38.0	280.0	22.7	2.23×10^{-12}	0.29
K6	38.0	293.0	22.5	2.54×10^{-12}	0.35
P1	37.8	76.3	16.1	1.01×10^{-14}	0.21
P2	37.9	76.3	19.6	1.37×10^{-14}	0.25
P3	38.3	205.0	19.8	1.52×10^{-14}	0.24
P4	38.0	205.0	20.0	6.51×10^{-15}	0.22
P5	38.0	280.0	19.5	1.82×10^{-14}	0.36
P6	38.0	282.0	19.0	3.50×10^{-14}	0.26

and the imbibition process is the quickest, 5 points per second for Estaillades and 2 points per second for Portland.

After imbibition has finished, we weigh the core again and by that we can measure the residual gas saturation (S_{gr}) using material balance. We assume that since we run the experiments at ambient conditions there is no compression of the gas after it is trapped. We then vacuum saturate the cores for 24 h to make sure that there is no air in the system. Then we insert the core into the Hassler cell to measure the permeability where we keep injecting degassed brine until we reach a steady-state flow regime.

Finally, we take the core out and weigh it to measure the porosity using the mass balance technique. For consistency, we replicate each experiment with a core from the same block of the same size. Table 2, summarizes the properties of the cores used in the experiments.

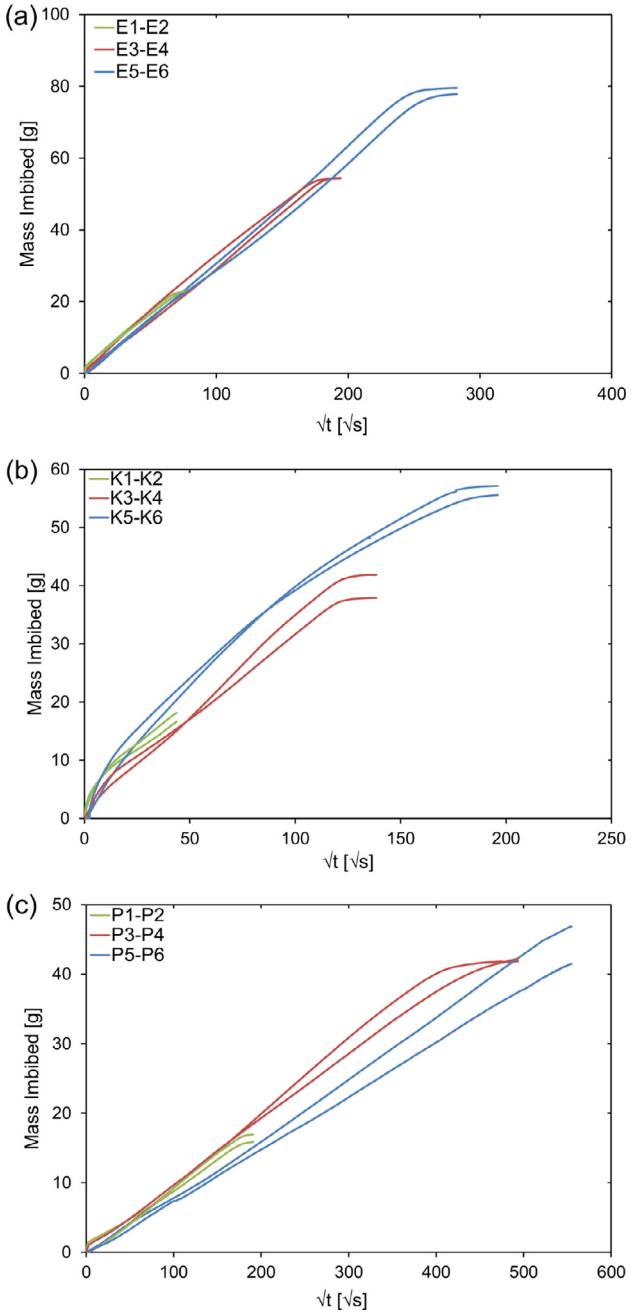

Fig. 4. Mass imbibed as a function of the square root of time for an air/brine system at ambient conditions of varying lengths for (a) Estaillades, (b) Ketton, and (c) Portland.

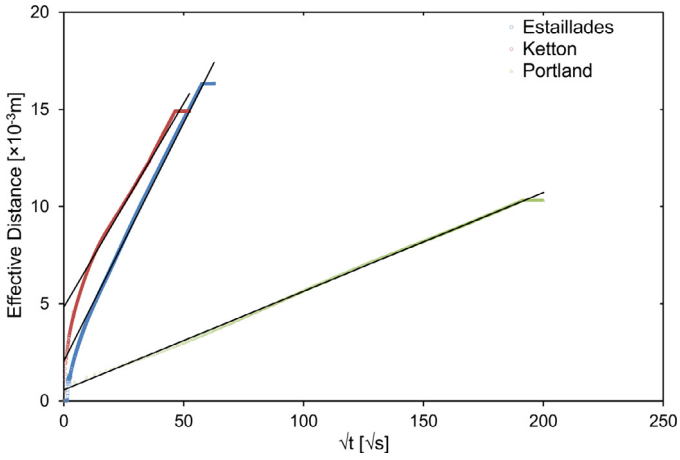

Fig. 5. The final step in the analysis is dividing the volume by the area and taking the slope. Noting that the slope is equivalent to $2C$ from Eq. (4) where we need to divide the slope by 2. The black lines are the slopes for each rock after the meniscus jump. Here the results for the shortest cores cores E1, K1, and P1 are shown; the sharp rise at the earliest time is a meniscus jump which is ignored in the analysis as well as the late time.

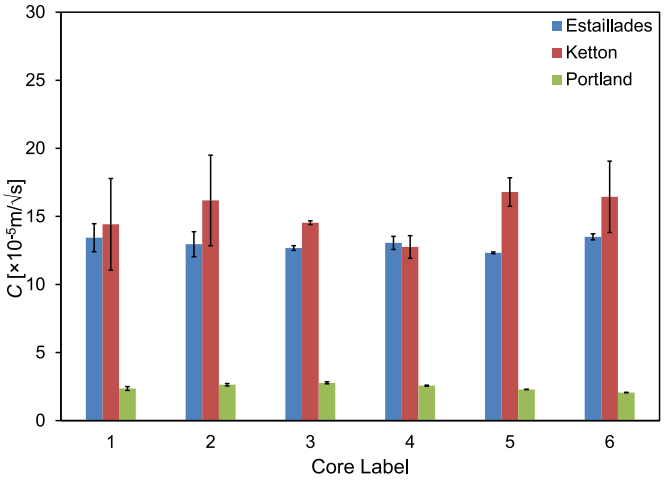

Fig. 6. The C values from the mass imbibition data for all the rocks in Table 2/Fig. 4.

3. Results and discussion

Fig. 4 shows the mass imbibed as a function of square root of time of the various lengths of each rock. We can see that the early imbibition shows a rapid increase of brine flow rate which then decays at a later time.

To find the value of C, which is the parameter that quantifies the rock's ability to imbibe we plot the mass imbibed as a function of $\sqrt{t}$ instead of t. We divide the mass imbibed by the brine density and by the area of the core open to water flow to obtain a volume per unit area; then by taking the slope of the curves we obtain the parameter $2C$ [m/$\sqrt{s}$], from Eq. (4), Fig. 5.

We see a sudden rise in the mass imbibed at the beginning of the experiment. This affects high permeability rocks more which is caused by a meniscus jump when the core is first put in contact with the brine (Lababjos-Broncano et al., 2001; Washburn, 1921). Other possible origins of this affect include an imbibition incubation time, or non-equilibrium effects: see Barenblatt et al. (1990, 2003) for a fuller discussion. We take the slope after this jump to find C–see Fig. 5. At a later time, when the water reaches the end of the core, again we can see a deviation from $\sqrt{t}$ scaling–this is ignored in our calculation of C. We can see that the estimated value of C is roughly constant regardless of the length of the core, Fig. 6. The error bars in this plot indicate the uncertainty from ignoring the meniscus jump region: they show the range of different slopes possible from the results.

The insensitivity of the results to core length implies that gravitational forces are negligible in these experiments. The gravitational pressure drop across the core is at most $\Delta\rho$gL where $\Delta\rho$ is the density contrast, g is the acceleration due to gravity, and L is the length of the core. This is at most 2,985 Pa for the largest cores. For comparison the air entry capillary pressure derived from the MICP measurements is 5,515 Pa, 3,447 Pa, and 33,784 Pa for Estaillades, Ketton, and Portland respectively: in all cases the capillary pressure is larger than the gravitational pressure difference. Although the gravitational pressure difference does have contribu-

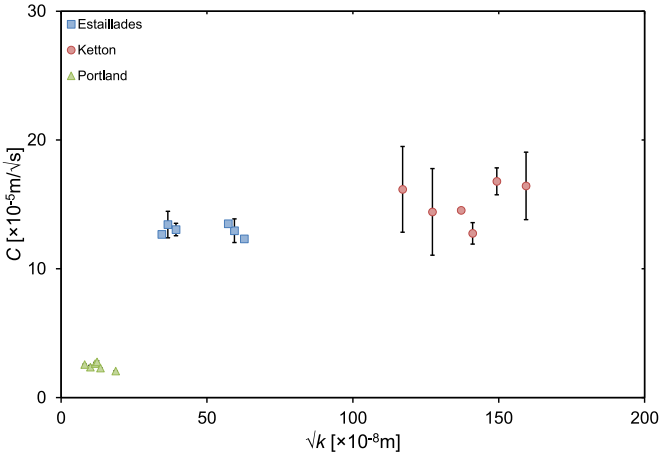

Fig. 7. Relationship between C, giving the rate of imbibition, and the square root of permeability $\sqrt{k}$ for all the rocks.

tion to the flow, we have ignored it in our analysis for the purpose of simplicity.

From Darcy's law, the flow rate is proportional to permeability k. However, here the driving force is capillary pressure, which using the Leverett J-function equation scales as $1/\sqrt{k}$:

$$P_c = \sigma \cos\theta \sqrt{\frac{\phi}{k}} J(S_w) \tag{6}$$

where P_c is capillary pressure [Pa], σ is interfacial tension [N/m], θ is the contact angle, ϕ is porosity, k is permeability [m^2], and $J(S_w)$ is the dimensionless J-function.

The end result is an imbibition rate that theoretically scales as $\sqrt{k}$. From the non-linear capillary dispersion, Eq. (3), we expect the rate at which the mass is imbibed, indicated by the parameter C, to scale as the square root of permeability, $\sqrt{k}$, as discussed previously. Fig. 7 shows the C plotted as a function of $\sqrt{k}$ for the three rocks. The rock type with the largest permeability - Ketton - tends to have the highest imbibition rate, while the lowest permeability rock - Portland - have the lowest rate.

Several studies have estimated relative permeability and capillary pressure from spontaneous imbibition measurements (Alyafei et al., 2016; Haugen et al., 2014; Li and Horne, 2005). In this paper, we show that we can estimate the relative permeability and capillary pressure from matching the semi-analytical solution with the experimental data. We compare the volume imbibed from the experiments and the semi-analytical solution. For this comparison, we use data for one rock of each type (E2, K1, P2) as shown in Fig. 8. Therefore, we use the C value to calculate the volume imbibed, which is described in Eq. (4) and multiplied by the area of the core sample used.

The calculation of the volumes imbibed are based on the C values from the semi-analytical solution: 14.2×10^{-5} m/$\sqrt{s}$, 16.1×10^{-5} m/$\sqrt{s}$, and 2.7×10^{-5} m/$\sqrt{s}$ for Estaillades, Ketton, and Portland respectively.

In our theoretical analysis we assume Corey or power-law expressions for relative permeability and capillary pressure:

$$k_{rw} = k_{rw,max}\left(\frac{S_w - S_{wi}}{1 - S_{wr} - S_{gr}}\right)^n \tag{7}$$

where k_{rw} is the water relative permeability, $k_{rw,\,max}$ is the maximum water relative permeability, S_w is the water saturation, S_{wi} is the initial water saturation, S_{gr} is the residual gas saturation, and n is the Corey water exponent.

$$k_{rg} = k_{rg,max}\left(\frac{1 - S_w - S_{wi}}{1 - S_{wr} - S_{gr}}\right)^m \tag{8}$$

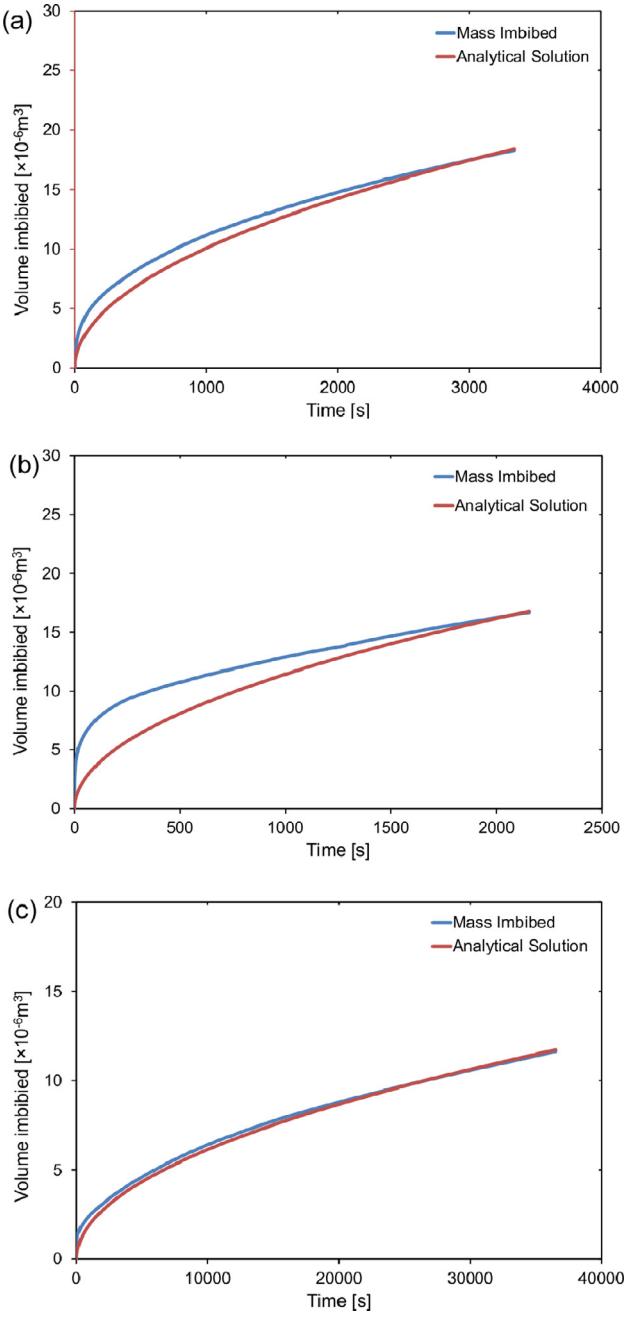

Fig. 8. Volume of water imbibed as a function of time from the mass imbibition experiments, cores (E2, K1, P2) are selected from Fig. 4 and calculation of the water volume imbibed based on the C values from the semi-analytical solution for (a) Estaillades, (b) Ketton, and (c) Portland.

where k_{rg} is the gas relative permeability, $k_{rg,\,max}$ is the maximum gas relative permeability, S_w is the water saturation, S_{wi} is the initial water saturation, S_{gr} is the residual gas saturation, and m is the Corey gas exponent.

$$P_c = P_{c,entry}\left(\frac{S_w - S_{wi}}{1 - S_{wi} - S_{gr}}\right)^{\alpha} \tag{9}$$

where P_c is the capillary pressure, $P_{c,\,entry}$ is the entry capillary pressure [Pa], S_w is the water saturation, S_{wi} is the initial water saturation, S_{gr} is the residual gas saturation, and α is the capillary pressure exponent.

Then, we adjust the following parameters: $k_{rw,\,max}$, n, $k_{ro,\,max}$, m, $P_{c,\,entry}$, and α so that the experimental results and analytical pre-

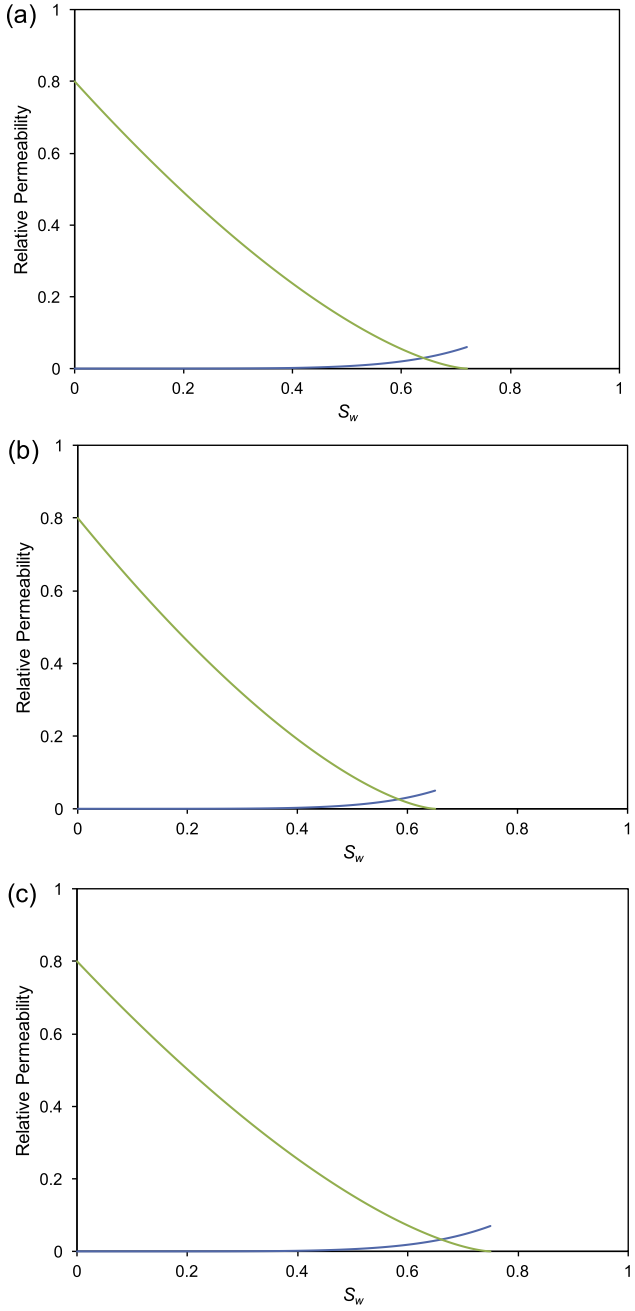

Fig. 9. Relative permeabilities used to match the semi-analytical solution with the experimental data in Fig. 8 for (a) Estaillades, (b) Ketton, and (c) Portland.

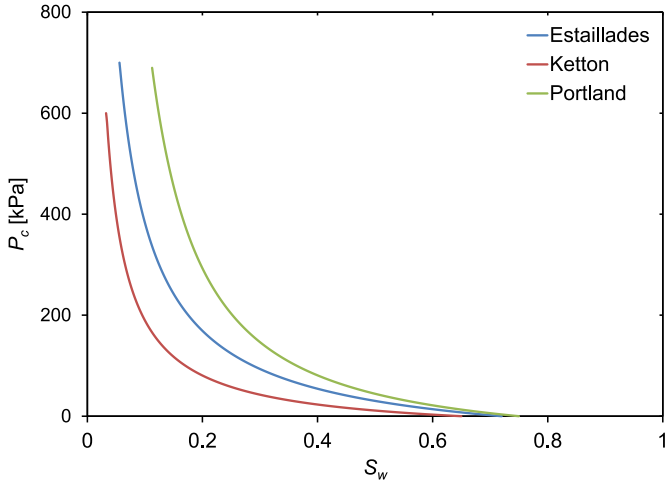

Fig. 10. Capillary pressures used to match the semi-analytical solution with the experimental data in Fig. 8 for the three rocks.

dictions match. The original spreadsheets were modified to handle mass imbibition and the updated version can be found here.

We found that the water relative permeability and capillary pressure have the most impact on the theoretical solution, while the air relative permeability had little impact on the results. This makes physical sense as the air has a low viscosity and is easily displaced–the movement of the water front is essentially controlled entirely by the water relative permeability (the ability to flow) and the capillary pressure (the driving force). Our best match is when the k_{rw} exponent ≥ 6. Since the core is initially dry, the water relative permeability is low, as water will first preferentially fill the largely immobile micro-porosity, giving a large change in saturation but little increase in relative permeability, indicative of a high Corey exponent. The relative permeabilities and capillary pressures used for the matching are shown in Figs. 9 and 10 respectively. The water saturation will have to increase to a large value in order to gain conductivity through the macro-porosity (Fernøet al., 2013). The presence of an initial water saturation may provide better conductivity with smaller Corey exponents (Li et al., 2002; Zhou et al., 2000).

The mass imbibition and the theoretical solution do not show good agreement with Ketton due to the meniscus jump. Our aim for this case is to match the mid-time recovery to avoid the uncertainty with the meniscus jump at the early time of imbibition. The matching becomes better as the permeability decreases. Further studies in improving experimental procedure to reduce the meniscus jump effect needs to be addressed. Overall, when matching the experimental data with the semi-analytical solution, the C values are in agreement with the experimental C values within experimental error.

The solution is not unique since we have only one measured function and three saturation-dependent properties–two relative permeabilities and the imbibition capillary pressure. However, these experiments could be used in conjunction with traditional coreflooding to determine all three functions together. For instance, if we had measured the two relative permeability functions, we should be able to find - uniquely - the capillary pressure that gave the measured imbibition profile. Hence, by using conventional measurements of relative permeability (steady-state or using Buckley–Leverett theory in an unsteady-state experiment) and the spontaneous imbibition saturation profile and/or mass imbibition data, we can measure the imbibition capillary pressure. We could also determine the imbibition relative permeability from a measured capillary pressure and the spontaneous imbibition data. As it stands, we can match the data but the functions used are not uniquely determined. Furthermore, this approach is only possible if we see $\sqrt{t}$ scaling of the imbibition front: a different method is needed if this is not the case (Nooruddin and Blunt, 2016).

4. Conclusions

We have used the solution for spontaneous imbibition derived by Schmid et al. (2011), to compare to direct experimental measurements and have shown its current applications and discussed its potential future applications. We have shown how to obtain the constant C, which determines the imbibition rate, from a simple mass imbibition experiment which is an important input parameter in the solution. We show that regardless of the length of the core, the measured value of C appears to be constant. The value is a function of permeability with higher C values for higher per-

meability rocks. We also show how to estimate imbibition relative permeability and capillary pressure from mass imbibition experiments. These estimations are not unique as we deal with several unknowns; however, we used reasonable estimate of relative permeability and capillary pressure as well as constraining the *C* values to experimental measurements. Future work could use measured saturation profiles using different fluid pairs and boundary conditions during imbibition to further help constrain the relative permeabilities and capillary pressures.

Acknowledgments

We would like to acknowledge the Qatar Carbonates and Carbon Storage Research Centre, QCCSRC, which is supported jointly by Qatar Petroleum, Shell and the Qatar Science & Technology Park and Qatar National Research Fund, QNRF, project number NPRP10-0101-170086 for funding this project.

References

Alyafei, N., Al-Menhali, A., Blunt, M.J., 2016. Experimental and analytical investigation of spontaneous imbibition in water-wet carbonates. Transp. Porous Media 115, 189–207. https://doi.org/10.1007/s11242-016-0761-4.

Alyafei, N., Blunt, M.J., 2016. The effect of wettability on capillary trapping in carbonates. Adv. Water Resour. 90, 36–50. https://doi.org/10.1016/j.advwatres.2016.02.001.

Ashton, M., 1980. The stratigraphy of the lincolnshire limestone formation (bajocian) in lincolnshire and rutland (leicestershire). Proc. Geol. Assoc. 91, 203–223. https://doi.org/10.1016/S0016-7878(80)80040-X.

Barenblatt, G.I., Entov, V.M., Ryzhik, V.M., 1990. Theory of Fluid Flows Through Natural Rocks. Kluwer Academic Publishers, Dordrecht, The Netherlands.

Barenblatt, G.I., Patzek, T.W., Silin, D.B., 2003. The mathematical model of nonequilibrium effects in water-oil displacement. SPE J. 8, 409–416. https://doi.org/10.2118/87329-PA.

Brenchley, P.J., Rawson, P.F., 2006. The geology of England and Wales. The Geological Society, London.

Cil, M.J.C.R., 1996. A multi-dimensional, analytical model for counter-current water imbibition into gas-saturated matrix blocks. J. Pet. Sci. Eng. 16, 61–69. https://doi.org/10.1016/0920-4105(95)00055-0.

Fernø, M.A., Haugen, r., Wickramathilaka, S., Howard, J., Graue, A., Mason, G., Morrow, N.R., 2013. Magnetic resonance imaging of the development of fronts during spontaneous imbibition. J. Pet. Sci. Eng. 101, 1–11. https://doi.org/10.1016/j.petrol.2012.11.012.

Graue, A., Fernø, M., 2011. Water mixing during spontaneous imbibition at different boundary and wettability conditions. J. Pet. Sci. Eng. 78, 586–595. https://doi.org/10.1016/j.petrol.2011.07.013.

Haugen, r., Fernø, M.A., Mason, G., Morrow, N.R., 2014. Capillary pressure and relative permeability estimated from a single spontaneous imbibition test. J. Pet. Sci. Eng. 115, 66–77. https://doi.org/10.1016/j.petrol.2014.02.001.

Kashchiev, D., Firoozabadi, A., 2003. Analytical solutions for 1d countercurrent imbibition in water-wet media. SPE J. 8. https://doi.org/10.2118/87333-PA.

Lababjos-Broncano, L., González-Martín, M.L., Braque, J.M., González-García, C.M., 2001. Influence of the meniscus at the bottom of the solid plate on imbibition experiments. J. Colloid Interf. Sci. 234 (1), 79–83. https://doi.org/10.1006/jcis.2000.7244.

Li, K., Chow, K., Horne, R.N., 2002. Effect of initial water saturation on spontaneous water imbibition. In: Proceedings of SPE Western Regional/AAPG Pacific Section Joint Meeting, May, Anchorage, Alaska, SPE-76727-MS, pp. 20–22. https://doi.org/10.2118/76727-MS.

Li, K., Horne, R.N., 2001. Characterization of spontaneous water imbibition into gas-saturated rocks. SPE J. 6, 375–384. https://doi.org/10.2118/74703-PA.

Li, K., Horne, R.N., 2005. Extracting capillary pressure and global mobility from spontaneous imbibition data in oil-water-rock systems. SPE J. 10, 458–465. https://doi.org/10.2118/80553-PA.

Lide, D.R., 2004. CRC Handbook of Chemistry and Physics. CRC.

Mason, G., Morrow, N.R., 2013. Developments in spontaneous imbibition and possibilities for future work. J. Pet. Sci. Eng. 110, 268–293. https://doi.org/10.1016/j.petrol.2013.08.018.

McWhorter, D.B., Sunada, D.K., 1990. Exact integral solutions for two-phase flow. Water Resour. Res. 26, 399–413. https://doi.org/10.1029/WR026i003p00399.

McWhorter, D.B., Sunada, D.K., 1992. Exact integral solutions for two-phase flow: reply. Water Resour. Res. 25 (1479). https://doi.org/10.1029/92WR00474.

Morrow, N.R., Mason, G., 2001. Recovery of oil by spontaneous imbibition. Curr. Opin. Colloid Interf. Sci. 6, 321–337. https://doi.org/10.1016/S1359-0294(01)00100-5.

Nooruddin, H.A., Blunt, M.J., 2016. Analytical and numerical investigations of spontaneous imbibition in porous media. Water Resour. Res 52. https://doi.org/10.1002/2015WR018451.

Olafuyi, O.A., Cinar, Y., Knackstedt, M.A., Pinczewski, W.V., 2007. Spontaneous imbibition in small cores, proceedings of the asia pacific oil and gas conference and exhibition. Jakarta, Indonesia, SPE-109724-MS, 30 October-1 November. https://doi.org/10.2118/109724-MS.

Schmid, K., Alyafei, N., Geiger, S., Blunt, M.J., 2016. Analytical solutions for spontaneous imbibition: fractional flow theory and experimental analysis. SPEJ 21. https://doi.org/10.2118/184393-PA.

Schmid, K.S., Geiger, S., Sorbie, K.S., 2011. Semianalytical solutions for cocurrent and countercurrent imbibition and dispersion of solutes in immiscible two-phase flow. Water Resour. Res. 47. https://doi.org/10.1029/2010WR009686. W02550.

Suzanne, K., Hamon, G., Billiotte, J., Trocme, V., 2003. Experimental relationships between residual gas saturation and initial gas saturation in heterogeneous sandstone reservoirs. In: Proceedings of the SPE Annual Technical Conference and Exhibition, pp. 5–8. https://doi.org/10.2118/84038-MS. October, Denver, Coloradol, SPE-84038-MS.

Tavassoli, Z., Zimmerman, R.W., Blunt, M.J., 2005. Analysis of counter-current imbibition with gravity in weakly water-wet systems. J. Pet. Sci. Eng. 48, 94–104. https://doi.org/10.1016/j.petrol.2005.04.003.

Washburn, E.W., 1921. The dynamics of capillary flow. Phys. Rev. 17 (3), 273–283. https://doi.org/10.1021/ef060456n.

Wright, V.P., Platt, N.H., Marriott, S.B., Beck, V.H., 1995. A classification of rhizogenic (root-formed) calcretes, with examples from the upper jurassic-lower cretaceous of spain and upper cretaceous of southern france. Sediment. Geol. 100, 143–158. https://doi.org/10.1016/0037-0738(95)00105-0.

Zhang, X., Morrow, N.R., Ma, S., 1996. Experimental verification of a modified scaling group for spontaneous imbibition. SPE Reserv.Eng. 11, 280–285. https://doi.org/10.2118/30762-PA.

Zhou, X., Morrow, N.R., Ma, S., 2000. Interrelationship of wettability, initial water saturation, aging time, and oil recovery by spontaneous imbibition and waterflooding. SPE J. 5, 199–207. https://doi.org/10.2118/62507-PA.